Calculation of Drag Coefficient for Arrays of Emergent Circular Cylinders with Pseudofluid Model

Nian-Sheng Cheng[1]

Abstract: The emergent vegetation in open-channel flows is usually simulated using arrays of circular cylinders in laboratory experiments. Analysis of recent experimental data reveals that for a given Reynolds number, the drag coefficient of a cylinder in a dense array is larger than that of an isolated cylinder. A new approach is applied to parameterize the drag coefficient and Reynolds number for flows through arrays of emergent cylinders. The approach is developed based on the concept of pseudofluid, for which an analogy is made between the cylinder-induced drag in an open-channel flow and that induced by the cylinder settling in a stationary fluid. With the proposed parameterization, the experimental database is successfully reorganized in such a way that a generalized drag coefficient is related to a generalized Reynolds number by one single curve, which is valid for a wide range of solid fractions and Reynolds numbers. However, it should be mentioned that only rigid circular stems are considered in this study and their induced drag is assumed to be dominant in comparison with the channel bed resistance. **DOI: 10.1061/(ASCE)HY.1943-7900.0000722.**

CE Database subject headings: Vegetation; Drag (fluid dynamics); Viscosity; Experimentation; Cylinders.

Author keywords: Vegetation; Cylinder; Drag coefficient; Reynolds number; Apparent viscosity; Open-channel flow; Pseudofluid model.

Introduction

The presence of vegetation in rivers and wetlands could influence various physical and biological processes in aquatic environments (James et al. 2004; Jordanova and James 2003; Kouwen et al. 1969; Luhar et al. 2008; Nepf et al. 2007). For example, the vegetation-induced resistance (Baptist et al. 2007; Cheng 2011; Huthoff et al. 2007; Stone and Shen 2002) may modify velocity profiles (Cheng et al. 2012), reduce flow discharges, and enhance flood attenuation and sediment deposition (Kothyari et al. 2009a). In laboratory studies, vegetation stems can be conveniently simulated with cylinder arrays. The flow through such cylinders is more complex than that around an isolated cylinder because of eddy–eddy and eddy–cylinder interactions (Nepf 1999; Zdravkovich 1997).

For an isolated cylinder subject to a uniform cross flow, there is plenty of information available in the literature on the evaluation of the induced drag (Kundu et al. 2004; Zdravkovich 1997). The drag coefficient decreases generally with the Reynolds number defined based on the cylinder diameter and the approach flow velocity. In the presence of other neighboring cylinders, the drag coefficient would also vary with cylinder spacing or stem fraction (i.e., the fraction of the stem-occupied channel bed area) in the vegetated open-channel flows (Cheng and Nguyen 2011; Kothyari et al. 2009b; Tanino and Nepf 2008). Ishikawa et al. (2000) reported that the change in the drag coefficient is significant but its dependence on the Reynolds number is not clear. Kothyari et al.'s (2009b) results indicate that the drag coefficient slightly varies with the Reynolds number but increases clearly with increasing stem fraction. Tanino and Nepf (2008) stated that the normalized drag, i.e., the ratio of the mean drag per unit cylinder length to the product of the viscosity and pore velocity, has a linear dependence on the Reynolds number. Cheng and Nguyen (2011) reported that the vegetation-based hydraulic radius can be used as a more reasonable length scale to describe the flow domain obstructed by the vegetation stems, which yields a redefined Reynolds number and thus an improved drag coefficient relationship.

All these previous studies show that the drag coefficient obtained for the cylinder array cannot be taken to be that applicable for a single isolated cylinder if the stem fraction is not small. However, how the single-cylinder drag coefficient is modified in the presence of other neighboring cylinders remains challenging at present, which is largely due to the poor understanding of complex vortex interactions among the cylinders (Sumer and Fredsøe 1997; Zdravkovich 1997). For example, Cheng and Nguyen (2011) have demonstrated that the vegetation-based hydraulic radius is a useful parameter to measure the length scale of the space among the stems. However, for the very sparse case, their derived drag coefficient cannot be explicitly reduced to that applicable for an isolated cylinder.

This paper extends the effort of Cheng and Nguyen (2011) by investigating how the drag coefficient used for a single isolated cylinder is modified by the presence of other neighboring cylinders. The objective is not to investigate details of the flow dynamics such as flow separation and vortex shedding in the presence of multiple cylinders. Rather, the dependence of the drag coefficient on the vegetation fraction is analyzed in an indirect approach. For an isolated cylinder subject to a cross flow, the functional relationship between the drag coefficient and Reynolds number is well established. Whether it is possible to extend the relationship to a cylinder in a dense array is investigated in the present study. The analysis conducted in this paper is based on the concept of pseudofluid, which yields a new parameterization of the drag coefficient.

Successful applications of the pseudofluid model can be found in the description of characteristics of various particle–fluid mixtures, for example, in studying fluidization (Gibilaro 2001) and the

[1]School of Civil and Environmental Engineering, Nanyang Technological Univ., Nanyang Avenue, Singapore 639798. E-mail: cnscheng@ntu.edu.sg

Note. This manuscript was submitted on January 5, 2012; approved on December 17, 2012; published online on December 19, 2012. Discussion period open until November 1, 2013; separate discussions must be submitted for individual papers. This paper is part of the ***Journal of Hydraulic Engineering***, Vol. 139, No. 6, June 1, 2013. © ASCE, ISSN 0733-9429/2013/6-602-611/$25.00.

transport of high-concentrated sediment (Wan and Wang 1994). With the apparent density and viscosity of the mixture, Cheng (1997) shows that the hindered settling velocity of sediment particles could be well estimated based on the drag coefficient derived for a single particle settling in a clear fluid. In the present study, a similar approach is developed to estimate the drag coefficient for cylinder-simulated vegetation stems for the emergent case. However, it should be mentioned that being different from the previous pseudofluid works, this study does not involve any physical investigation of the settling phenomena. Instead, a connection is established between the energy slope observed in the vegetated open-channel flow and the relative density involved necessarily in the settling phenomena. With this connection, all parameters used in the pseudofluid model are shown physically measurable for open-channel flows subject to emergent cylinders.

This paper is outlined as follows: First, an empirical formula is proposed to represent the classical relationship between the drag coefficient and Reynolds number for an isolated cylinder subject to a cross flow. Then, to extend this formula to the vegetated open-channel flow, a pseudofluid model is established. Finally, various experimental data available in the literature for a wide range of vegetation configurations are unified with a generalized drag coefficient and a generalized Reynolds number that apply for both cases of isolated cylinder and cylinder array. All the analyses conducted in this paper are limited to circular rigid cylinders that are present in open-channel flows under the emergent condition.

Drag Coefficient for an Isolated Cylinder

When being subject to a uniform cross flow, an isolated cylinder may induce a variation of drags, depending on its diameter d, the approach flow velocity V, and the kinematic viscosity of fluid ν. This variation is closely associated with different flow separation phenomena around the cylinder (Kundu et al. 2004; Niemann and Holscher 1990; Williamson 1996; Zdravkovich 1997). Several classical data sets have been reported in the literature on the drag coefficient C_D for isolated circular cylinders. Examples are those provided by Wieselsberger (1922), Finn (1953), Tritton (1959), and Jayaweera and Mason (1965). All these data are plotted in Fig. 1, where $C_D = 2F_D/(\rho d V^2)$, F_D is the average drag exerting on the cylinder per unit length, ρ is the density of fluid, and $\mathsf{R}(= Vd/\nu)$ is the Reynolds number.

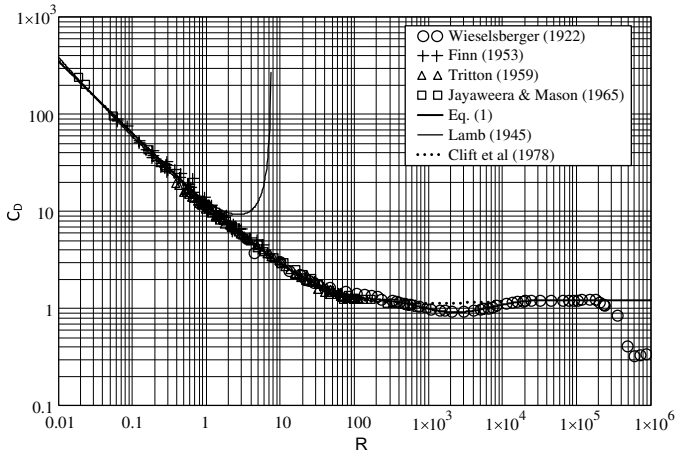

Fig. 1. Variation of drag coefficient $[C_D = 2F_D/(\rho d V^2)]$ with Reynolds number $(\mathsf{R} = Vd/\nu)$ for a single isolated cylinder subject to a cross flow

Also plotted in Fig. 1 are some empirical formulas proposed to describe the variation of the drag coefficient. The previous formulas apply only for a limited range of Reynolds number. For example, the formula by Clift et al. (1978) applies for $0.1 < \mathsf{R} < 400$, while the one by Lamb (1945) is used for $\mathsf{R} < 1$. In this study, the following empirical formula is proposed to represent the data for a wider range of Reynolds numbers (i.e., $\mathsf{R} = 0.02 - 2 \times 10^5$) (see Fig. 1):

$$C_D = 11\mathsf{R}^{-0.75} + 0.9\left[1 - \exp\left(-\frac{1{,}000}{\mathsf{R}}\right)\right] + 1.2\left[1 - \exp\left(-\left(\frac{\mathsf{R}}{4{,}500}\right)^{0.7}\right)\right] \quad (1)$$

The functional relationship of C_D-R shown in Eq. (1) or Fig. 1 applies to an isolated cylinder subject to a cross flow. Whether it is possible to extend the application to a cylinder in a dense array is explored subsequently in this paper. The flow configuration associated with Eq. (1) is sketched in Fig. 2(a), where the flow velocity of the cross flow is V, the dashed box denotes the entire cylinder, and the shaded area denotes the segment with a unit length. It is assumed that the length of the cylinder is much greater than its diameter and the end effect is negligible. To appreciate how the drag varies with V, one may alternatively consider the cylinder settling in a stationary fluid [see Fig. 2(b)]. It is assumed in this paper that the cylinder remains horizontal when settling in velocity V. Such a settling fashion may not be true because the cylinder may tumble in the fluid. However, what is concerned in this paper is the equivalence of the different drags experienced by the cylinder under the two different conditions, rather than the detail of the settling phenomena. With the density difference between the cylinder and the fluid, the drag could be measured as the effective weight of the cylinder per unit length. This drag would be the same as that for the case of Fig. 2(a) because of the same relative velocity. If the density of the cylinder is ρ_s, the effective weight W per unit length is

$$W = \frac{\pi d^2}{4}(\rho_s - \rho)g \quad (2)$$

By taking $F_D = W$ and noting that $F_D = C_D \rho d V^2/2$, one gets

$$C_D = \frac{\pi}{2}\frac{\Delta d g}{V^2} \quad (3)$$

where $\Delta[= (\rho_s - \rho)/\rho]$ is the relative density difference. With the analogy made, this drag coefficient should be equivalent to the C_D

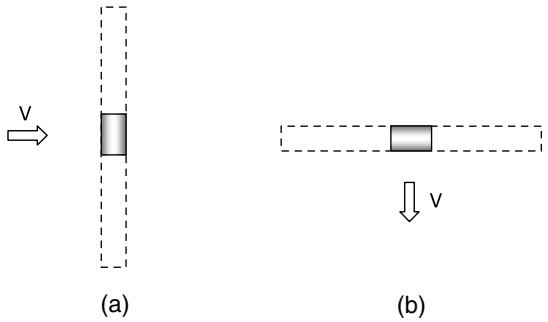

Fig. 2. (a) Vertical cylinder subject to horizontal cross flow with velocity V; (b) horizontal cylinder settling with velocity V in a stationary fluid; the dashed box denotes the entire cylinder and the shaded area denotes the segment of unit length

J. Hydraul. Eng., 2013, 139(6): 602-611

used for the case of Fig. 2(a), both being defined based on the same drag.

Furthermore, using the C_D given in Eq. (3), a dimensionless cylinder diameter d_* can be defined as follows:

$$d_* = \left(\frac{2}{\pi} C_D \mathsf{R}^2\right)^{1/3} = \left(\frac{\Delta g}{\nu^2}\right)^{1/3} d \tag{4}$$

From Eq. (4), it follows that $\mathsf{R} = \sqrt{\pi d_*^3/(2C_D)}$. If substituting this into Eq. (1), the relationship between C_D and d_* can be established but the result cannot be expressed in an explicit function. On the other hand, it is observed that C_D varies with d_* in a fashion very similar to that shown in Fig. 1. Therefore, the following formula, in the form similar to Eq. (1), is proposed to describe the variation of C_D with d_* for $d_* = 0.3 - 3{,}300$

$$C_D = 35 d_*^{-1.75} + 1.15\left[1 - \exp\left(-\frac{80}{d_*}\right)\right] + 1.2\left[1 - \exp\left(-\frac{d_*}{330}\right)\right] \tag{5}$$

As shown in Fig. 3, Eq. (5) represents well the experimental data, the same as those plotted in Fig. 1, with the values of d_* being calculated from C_D and R using Eq. (4). Eq. (5) shows that for a settling cylinder, C_D can be calculated with given Δ, d, and ν. In the subsequent analysis, Eq. (5) will be used to develop the pseudofluid model. However, it is noted that Δ is not a parameter physically applicable for vegetated open channel flows, but it can be expressed as a function of the energy slope, as derived in the next section.

Drag Acting on Cylinder Array

Now consider an array of cylinders that simulate the vegetation stems in an open-channel flow [Fig. 4(a)]. It is assumed that the array in the streamwise direction is long enough that the flow through the cylinders can be considered fully developed. Similar to the analysis presented in the preceding section, two scenarios are compared in this section. The first is an open-channel flow subject to an array of emergent rigid cylinders [see Fig. 4(a)]. The average energy slope of the flow is S, and the average flow velocity through the emergent vegetation is V_v. If the channel width

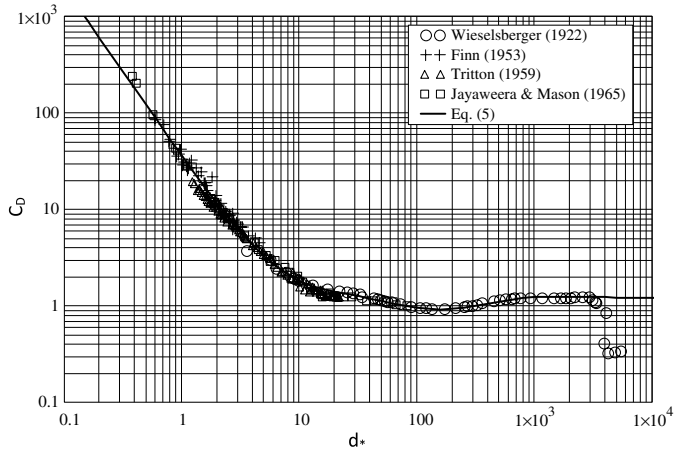

Fig. 3. Relationship between drag coefficient $C_D[= 2F_D/(\rho d V^2)]$ and dimensionless cylinder diameter $d_*[= (2C_D\mathsf{R}^2/\pi)^{1/3}]$ for a single isolated cylinder

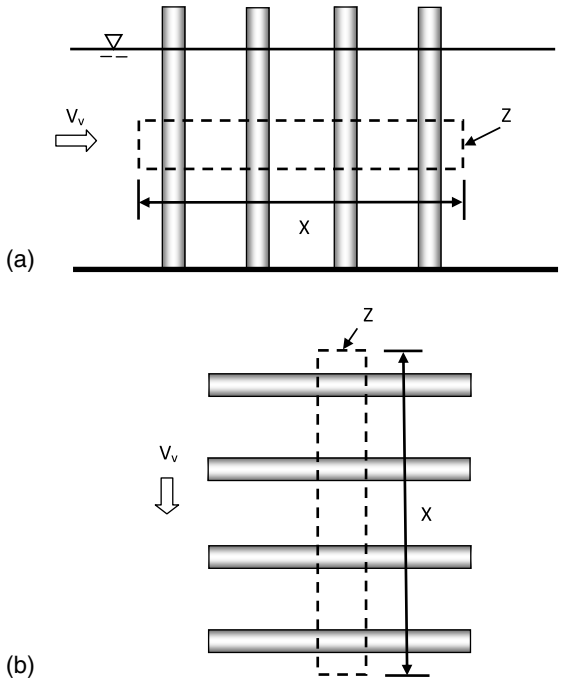

Fig. 4. (a) Vegetated open-channel flow; (b) settling of cylinder array, where the size of control volume is XYZ and Y is the dimension perpendicular to plane XZ but is not shown

is B, the flow depth is h, and the flow discharge is Q, V_v can be estimated as $Q/[Bh(1-\lambda)]$, where λ is the average solid fraction defined as the fraction of the stem-occupied bed area. This calculation is considered as an approximation, which is discussed in the appendix. If the drag coefficient denoted by C_{Da} is known for the cylinder array, the average drag acting on a cylinder per unit length is

$$F_{Da} = \frac{1}{2} C_{Da} \rho d V_v^2 \tag{6}$$

where the subscript a is used to denote the parameters related to the cylinder array. C_{Da} tends to C_D as λ becomes small.

Furthermore, a control volume is selected as shown in Fig. 4(a), of which the length, height, and width are X, Z, and Y, respectively. Y is the dimension measured in the direction perpendicular to plane XZ but is not shown in Fig. 4. In the control volume, the total number of the cylinders is $N = XY\lambda/(\pi d^2/4)$. Then, the average drag for a cylinder per unit length is equal to the corresponding streamwise component of the gravity of the fluid (Cheng and Chiew 1999), i.e.,

$$F_{Da} = \frac{XYZ\rho g S}{NZ} = \frac{XYZ\rho g S}{XYZ\lambda}\frac{\pi d^2}{4} = \frac{\pi d^2}{4}\frac{1}{\lambda}\rho g S \tag{7}$$

In this equation, the drag associated with the cylinders is considered dominant while the bed friction, sidewall friction, and the free surface effect are all negligible. In other words, the energy slope S is solely associated with the energy loss caused by the emergent cylinders. The energy slope in an open-channel flow is usually of the order of 1% at most. If it is very large, S in Eq. (7) should be replaced with $S/\sqrt{1+S^2}$ for describing precisely the streamwise component of the gravity. With Eqs. (6) and (7),

$$C_{Da} = \frac{\pi}{2}\frac{1}{\lambda}\frac{gdS}{V_v^2} \tag{8}$$

For the sparse vegetation, C_{Da} computed using Eq. (8) is expected to be the same as that given in Eq. (1) for a single isolated cylinder.

The second scenario is sketched in Fig. 4(b), where the cylinder array of the same configuration is placed horizontally. The cylinders settle in a stationary fluid and the settling velocity of the cylinders relative to the fluid is set at V_v, the same velocity as that for the case of Fig. 4(a). No wall boundary is presented in this case and thus the length of the individual cylinders is considered infinite. In terms of the cylinder size, spacing, and the relative velocity, both scenarios could be considered equivalent. However, the difference is that the first setup is often employed to experimentally investigate the vegetated open-channel flow, while the second scenario is imaginary and may not be reproduced in a simple experimental setup because of complex flow interactions among the cylinders. This imaginary model is purposely designed to facilitate the subsequent analysis, for which it is more important to know the connection between the two scenarios than details involved in the settling phenomenon, the latter being beyond the objective of this study.

For the control volume of the same size [as shown in Fig. 4(b)], the induced drag for each cylinder per unit length is equal to its effective weight,

$$F_{Da} = \frac{\pi d^2}{4}(\rho_s - \rho)g = \frac{\pi d^2}{4}\Delta\rho g \tag{9}$$

From Eq. (9), it is noted that the drag is proportional to the density difference. In other words, it is the density difference that results in the driving force for the settling cylinder. In comparison, in the first scenario [Fig. 4(a)], the driving force derives from the streamwise component of the gravity of the fluid, which can be quantified using the energy slope [see Eq. (7)].

By noting the equivalent drag assumed for the two scenarios, with Eqs. (6) and (9),

$$C_{Da} = \frac{\pi}{2}\frac{\Delta g d}{V_v^2} \tag{10}$$

Furthermore, because Eq. (10) is equivalent to Eq. (8), one gets

$$\Delta = \frac{S}{\lambda} \tag{11}$$

Eq. (11) provides the basic relationship between the relative density difference Δ and the energy slope S that connects the two scenarios under consideration. As mentioned previously, Δ serves as an important parameter to quantify the driving force for the settling cylinder, while S signifies the streamwise component of the fluid gravity per unit weight for the vegetated open-channel flow. Using the relationship given in Eq. (11), the effect of the energy slope on the flow velocity through the emergent vegetation in an open-channel flow could be appreciated by considering how the relative density difference influences the settling velocity of the cylinder array. With this result, whenever Δ is involved in the pseudofluid model proposed in the following section, it will be replaced with S/λ.

Pseudofluid Model

In studying the hindered settling in a sediment-fluid mixture, the drag coefficient could be well estimated using the formula that is proposed for the particle settling in a clear fluid (Cheng 1997). The idea developed for the pseudofluid model is to take the sediment–fluid mixture as a new fluid characterized with the apparent (or mixture) density and viscosity, which are different from those of the clear fluid and dependent on the sediment concentration in the mixture. In the present study, a similar idea is applied to explore a possible connection between the drag coefficient for an isolated cylinder and that for an array of cylinders. However, there is a difference between the present study and the previous work (Cheng 1997). In the previous pseudofluid model, the density of the particle or mixture is physically measurable. In comparison, in the present study, the so-called settling does not happen in reality. As a result, the relative density difference is first taken as an intermediate or temporary parameter in the analysis. Then the relative density difference is expressed as a function of the energy slope that is observed in vegetated open-channel flows, as given in Eq. (11).

For the settling of a single cylinder as shown in Fig. 2(b), the relationship between C_D and d_* is given in Eq. (5). For the settling of an array of cylinders as shown in Fig. 4(b), it is assumed that the same relationship applies, provided that the apparent density and viscosity are used. Therefore, Eq. (5) is rewritten as

$$C_D' = 35d_*'^{-1.75} + 1.15\left[1 - \exp\left(-\frac{80}{d_*'}\right)\right] + 1.2\left[1 - \exp\left(-\frac{d_*'}{330}\right)\right] \tag{12}$$

with

$$C_D' = \frac{\pi}{2}\frac{\Delta' dg}{V_v^2} \tag{13}$$

and

$$d_*' = \left(\frac{\Delta' g}{\nu'^2}\right)^{1/3} d \tag{14}$$

where the superscript $'$ denotes the parameters used for the cylinder-fluid mixture, ν' is the apparent kinematic viscosity, ρ' is the apparent density defined as

$$\rho' = \rho_s\lambda + \rho(1-\lambda) \tag{15}$$

and Δ' is the relative density difference of the mixture defined as

$$\Delta' = \frac{\rho_s - \rho'}{\rho'} \tag{16}$$

Eqs. (13) and (14) are counterparts of Eqs. (3) and (4). With Eqs. (15) and (16), it can be further shown that

$$\Delta' = \frac{(1-\lambda)\Delta}{1+\Delta\lambda} \tag{17}$$

Then Eq. (14) is rewritten to be

$$d_*' = \left[\frac{(1-\lambda)\Delta}{1+\Delta\lambda}\frac{g}{\nu_r^2\nu^2}\right]^{1/3} d \tag{18}$$

where $\nu_r (= \nu'/\nu)$ is the relative kinematic viscosity. If using the dynamic viscosity of the fluid (μ) and that of the mixture (μ'),

$$\nu_r = \frac{\mu'}{\mu}\frac{\rho}{\rho'} = \frac{\mu_r}{1+\Delta\lambda} \tag{19}$$

where $\mu_r(=\mu'/\mu)$ is the relative dynamic viscosity. Moreover, by noting that Δ is related to S [see Eq. (11)], Eq. (18) can be further expressed as

$$d'_* = \left(\frac{(1-\lambda)(1+S)S}{\lambda}\frac{g}{\mu_r^2\nu^2}\right)^{1/3} d \tag{20}$$

Similarly, using Eqs. (17) and (11), Eq. (13) can be rewritten to be

$$C'_D = \frac{\pi}{2}\frac{(1-\lambda)S}{\lambda+\lambda S}\frac{dg}{V_v^2} \tag{21}$$

In the form similar to Eq. (4), d'_* can be also related to C'_D using a Reynolds number,

$$d'_* = \left(\frac{2}{\pi}C'_D\mathsf{R}'^2\right)^{1/3} = \left(\frac{\Delta' g}{\nu'^2}\right)^{1/3} d \tag{22}$$

where $\mathsf{R}'(=V_v d/\nu')$ is the Reynolds number used in the pseudo-fluid model. From Eqs. (20) and (21), it is noted that both d'_* and C'_D are dependent on the vegetation configuration (stem diameter and fraction) and the energy slope, but they are not associated with the relative density difference. Using Eq. (20), d'_* can be determined if the five parameters (λ, d, S, ν, and μ_r) are known. Then, C'_D can be found with d'_* from Eq. (12) and V_v can be thus obtained using Eq. (21), i.e.,

$$V_v = \sqrt{\frac{\pi}{2}\frac{(1-\lambda)S}{\lambda+\lambda S}\frac{dg}{C'_D}} \tag{23}$$

Eqs. (12), (20), and (23) form the model system for the calculation of the flow velocity through the emergent vegetation. Among the five parameters, λ, d, S, and ν are usually available for particular vegetation configuration and flow condition employed in experimental studies. However, how to evaluate μ_r is not clear. This will be discussed next.

Apparent Dynamic Viscosity

In studying the particle–fluid mixture, the apparent viscosity is often expressed as a function of the particle concentration. As reviewed by Poletto and Joseph (1995) and Cheng and Law (2003), almost all such functions are empirical except for the one proposed by Einstein (1906) for the very low concentration. The differences among the empirical formulas appear very large for the particle concentration greater than 30%. However, they all imply that the relative dynamic viscosity varies almost linearly for the particle concentration less than 15% (Cheng and Law 2003; Gibilaro et al. 2007).

In this study, different forms of formulas have been tried to calculate μ_r, but as presented in the following section, the best calculation of V_v using Eq. (23) could be made with μ_r in the following linear form:

$$\mu_r = 1 + \alpha\lambda \tag{24}$$

where α is a constant. The coefficient α included in Eq. (24) is the only parameter that needs to be calibrated for the model proposed.

Model Calibration

Based on the preceding derivation, the procedure for calculating the average velocity through emergent, rigid, cylindrical stems is summarized as follows:

1. For a given λ, d, S, and ν, use Eqs. (20) and (24) to calculate d'_*. The constant α in Eq. (24) could be taken to be 80, as shown in the subsequent section.
2. Next find C'_D using Eq. (12).
3. Then calculate V_v with Eq. (23). The flow rate Q is calculated as $V_v Bh(1-\lambda)$.

To apply the proposed model, 396 data sets are used in this study (see Table 1), which include the laboratory measurements reported by Ishikawa et al. (2000), James et al. (2004), Liu et al. (2008), Tanino and Nepf (2008; personal communication, 2010), Ferreira et al. (2009), and Cheng and Nguyen (2011). The experiments by James et al. (2004) and Ishikawa et al. (2000) were conducted under the sand-bed condition, so the bed and sidewall corrections were made to their data.

The procedure of the correction is detailed in Cheng and Nguyen (2011). In this study, the same procedure is applied but with some slight changes. Cheng and Nguyen (2011) used the vegetation-related hydraulic radius $r_v[=(\pi/4)(1-\lambda)d/\lambda]$ for the calculation of the flow velocity through the emergent vegetation. To perform the bed and sidewall correction, r_v is modified to r_{vm},

$$r_{vm} = r_v\left[1 - \left(\frac{f_w}{0.5B(1-\lambda)} + \frac{f_b}{h}\right)\frac{r}{f}\right] \tag{25}$$

where f_b = bed−related friction factor; f_w = sidewall-related friction factor; B = channel width; h = flow depth; r = hydraulic radius defined as

$$r = \left(\frac{1}{h} + \frac{1}{0.5B(1-\lambda)} + \frac{1}{r_v}\right)^{-1} \tag{26}$$

and $f = 8grS/V_v^2$. By noting that r_v is proportional to d, the modification of r_v to r_{vm} can be made simply by replacing d with $(r_{vm}/r_v)d$.

The correction results show that the changes related to the data by James et al. (2004) and Ishikawa et al. (2000) are significant, while those for the other data are minor. No correction was made to the data by Tanino and Nepf (2008; personal communication, 2010) because some of the flow information is not available.

Table 1. Summary of Previously Collected Experimental Data

Investigator	Number of datasets	Vegetation fraction, λ	Stem arrangement	Stem diameter, d (mm)	$\mathsf{R}_a(V_v d/\nu)$
Ishikawa et al. (2000)	30	0.00314–0.0126	Staggered	4; 6.4	910–4,570
James et al. (2004)	23	0.0035–0.0314	Staggered	5	240–870
Liu et al. (2008)	9	0.0031–0.0160	Staggered; in-line	6.35	1,280–2,200
Tanino and Nepf (2008)	116	0.090–0.35	Random	6.4	25–690
Ferreira et al. (2009)	2	0.022–0.038	Random	11	1,190–1,450
Tanino and Nepf (personal communication, 2010)	73	0.031–0.056	Staggered	6.4	110–830
Cheng and Nguyen (2011)	143	0.0043–0.119	Staggered	3.2; 6.6; 8.3	200–1,540

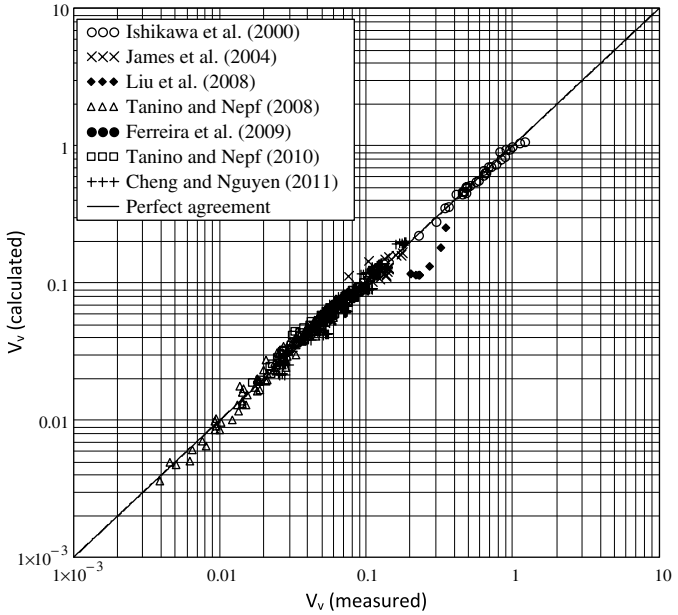

Fig. 5. Comparison of calculated and measured average velocities (m/s) through cylindrical stems, where the measured values were estimated from flow rates as $Q/[Bh(1-\lambda)]$

However, it is believed that the corrections would be negligible by noting the high vegetation fractions employed by Tanino and Nepf (2008).

Fig. 5 shows the calculated flow velocities in comparison with the measurements. In the calculation, the coefficient α [see Eq. (24)] was taken to be 80, which minimizes the residuals of calibration. Two statistical parameters are used to assess the goodness of the calibration. They are Err_1, the average value of the relative error, defined as $|\text{calculated } V_v - \text{measured } V_v|/(\text{measured } V_v)$, and Err_2, the average value of the squared deviation defined using the logarithmic velocity, which is calculated as $[\log(\text{calculated } V_v) - \log(\text{measured } V_v)]^2$. Table 2 summarizes the residuals for the seven sets of data. For all data sets except for those by Liu et al. (2008), the average values of Err_1 are not greater than 13.7%, while the values of Err_2 are not greater than 4.1×10^{-3}.

Variation of Drag Coefficient with Reynolds Number and Vegetation Fraction

Fig. 6 shows the variation of the $C_{Da} - \mathsf{R}_a$ relationship with the solid fraction, where C_{Da} is calculated as $\pi gdS/(2\lambda V_v^2)$, as given in Eq. (8), and R_a is calculated as $V_v d/\nu$. As expected, when λ is small, C_{Da} and R_a converge to C_D and R, respectively, the latter two parameters being used in Eq. (1) and Fig. 1. The curves plotted were calculated using the proposed model, i.e., Eqs. (12), (20), and (23), for a series of λ, i.e., 0.03, 0.1, 0.2, 0.3, and 0.4. For each particular λ, the calculation of V_v was conducted by varying S from 10^{-6} to 0.3 and taking $d = 0.006$ m and $\nu = 10^{-6}$ m^2/s.

Also plotted in Fig. 6 are Eq. (1) and the experimental data summarized in Table 1. Fig. 6 clearly shows how the drag coefficient for an isolated cylinder is modified by the presence of the other neighboring ones. It can be observed that the drag coefficient systematically increases with increasing stem fraction and significant changes occur at low Reynolds numbers even for low vegetation fractions. For example, for $\lambda = 0.03$, the drag coefficient appears to be very close to Eq. (1) for $\mathsf{R}_a > 100$, but starts to increase when R_a reduces. The calculation also confirms that the calculated curve for very small λ appears to be close to that calculated with Eq. (1).

Generally, the calculated curves for the different λ values are supported by the experiments in spite of the spreading of the data points. For example, for $\mathsf{R}_a < 100$, the data that were collected by Tanino and Nepf (2008) for $\lambda = 0.15 - 0.35$ are well confined by the two curves calculated for $\lambda = 0.2$ and 0.3, respectively. For $\mathsf{R}_a = 500 - 5{,}000$, the data points are in the range of $\lambda = 0.003 - 0.119$ and most of them appear below the calculated curve for $\lambda = 0.1$ but above the curve calculated with Eq. (1). For the calculation of the curves, d was taken to be 0.006 m, which is the average cylinder size employed in the experiments. Additional calculations show that the curves are not sensitive to the selection of d. When d varies from 0.003 to 0.011 m (the same range as in the data), the curves remain unchanged for low Reynolds numbers and vary slightly for high Reynolds numbers.

Table 2. Summary of Calibration Residuals

Investigator	Err_1 (%)	$\text{Err}_2(10^{-3})$
Ishikawa et al. (2000)	4.0	0.5
James et al. (2004)	11.1	3.8
Liu et al. (2008)	45.8	75.7
Tanino and Nepf (2008)	13.7	4.1
Ferreira et al. (2009)	8.3	1.6
Tanino and Nepf (unpublished, 2010)	8.6	2.0
Cheng and Nguyen (2011)	9.0	2.3

Generalized Drag Coefficient and Reynolds Number

In the foregoing sections, three pairs of drag coefficients and Reynolds numbers are defined, as summarized in Table 3. For a single isolated cylinder, C_D and R are defined based on the approach flow velocity and cylinder diameter, while for a typical cylinder in an array, C_{Da} and R_a are used by involving the average flow velocity through the stems. When the vegetation becomes sparse, C_{Da} and R_a reduce to C_D and R, respectively; otherwise, the relationship of C_{Da}-R_a varies with the vegetation fraction

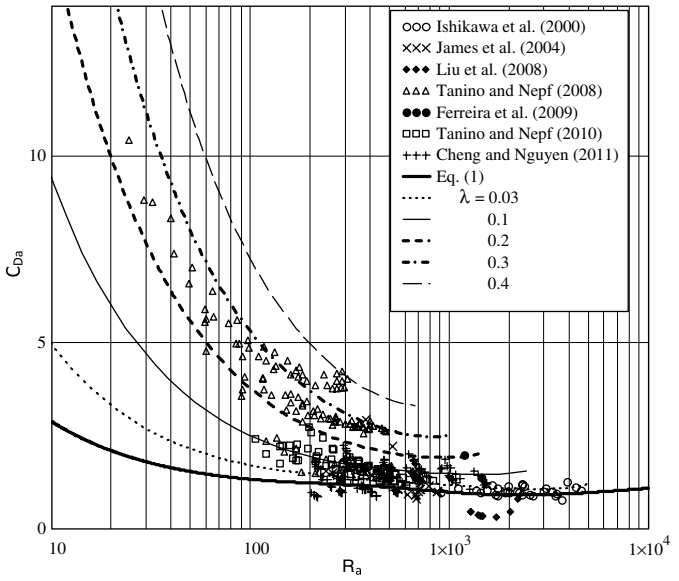

Fig. 6. Variations of drag coefficient $C_{Da}[= \pi gdS/(2\lambda V_v^2)]$ with Reynolds number $\mathsf{R}_a(= V_v d/\nu)$ and vegetation fraction λ

J. Hydraul. Eng., 2013, 139(6): 602-611

Table 3. Comparison of Different Drag Coefficients and Reynolds Numbers

Case	Reynolds number	Drag coefficient	Dimensionless cylinder diameter
Single isolated cylinder	$\mathsf{R} = \frac{Vd}{\nu}$	$C_D = \frac{2F_D}{\rho d V^2}$	$d_* = \left(\frac{2}{\pi} C_D \mathsf{R}^2\right)^{1/3}$
Cylinder array	$\mathsf{R}_a = \frac{V_v d}{\nu}$	$C_{Da} = \frac{2F_{Da}}{\rho d V_v^2} = \frac{\pi 1 g d S}{2\lambda V_v^2}$	$\left(\frac{2}{\pi} C_{Da} \mathsf{R}_a^2\right)^{1/3}$
Pseudofluid model	$\mathsf{R}' = \frac{V_v d}{\nu'} = \frac{1+S}{1+80\lambda}\mathsf{R}_a$	$C_D' = \frac{1-\lambda}{1+S} C_{Da}$	$d_*' = \left(\frac{2}{\pi} C_D' \mathsf{R}'^2\right)^{1/3}$

Note: $V_v = Q/Bh(1-\lambda)$; $\nu' = \mu_r \nu/(1+S)$; $\mu_r \approx 1 + 80\lambda$.

(see Fig. 6). In developing the pseudofluid model, the pair of dimensionless parameters are further replaced with C_D' and R'.

In this section, it is shown that C_D' and R' can be considered to be the generalized forms of C_D and R, respectively. First, with Eqs. (8) and (21), C_D' is rewritten to be

$$C_D' = \frac{1-\lambda}{1+S} C_{Da} \tag{27}$$

Obviously, with decreasing λ, C_D' converges to C_{Da} and then C_D for an isolated cylinder. Then, by noting that $\nu' = \mu'/\rho' = \mu_r \mu/\rho'$, $\rho'/\rho = 1 + \Delta\lambda$, $\Delta\lambda = S$ [see Eq. (11)], and $\mu_r = 1 + 80\lambda$ [see Eq. (24)], R' can be further expressed to be

$$\mathsf{R}' = \frac{1+S}{1+80\lambda}\mathsf{R}_a \tag{28}$$

It can be seen that with decreasing λ, R' reduces to R_a and then R for an isolated cylinder. Based on the concept of the pseudofluid, it has been shown that the function remains unchanged in describing the relationship of C_D-d_* [see Eq. (5)] and C_D'-d_*' [see Eq. (12)]. By considering that $d_* = (2C_D \mathsf{R}^2/\pi)^{1/3}$ [see Eq. (4)] and $d_*' = (2C_D' \mathsf{R}'^2/\pi)^{1/3}$ [see Eq. (22)], the functional relationship that is developed for C_D-R [i.e., Eq. (1)] should be also applicable for that of C_D'-R'. Therefore, Eq. (1) can be reformulated to be

$$C_D' = 11\mathsf{R}'^{-0.75} + 0.9\left[1 - \exp\left(-\frac{1{,}000}{\mathsf{R}'}\right)\right] + 1.2\left[1 - \exp\left(-\left(\frac{\mathsf{R}'}{4{,}500}\right)^{0.7}\right)\right] \tag{29}$$

The data summarized in Table 1 are used to calculate C_D' and R' by applying Eqs. (27) and (28), respectively. The results are plotted in Fig. 7. It can be observed that the data points do not group together according to the vegetation fraction (unlike those in Fig. 6). Instead, they can be reasonably represented by the sole solid line plotted according to Eq. (29), the same function as given in Eq. (1) between C_D and R for a single isolated cylinder.

The implications of this result are twofold. First, the relationship between C_D' and R', both parameters being derived with the pseudofluid consideration, is applicable to an isolated cylinder as well as a cylinder array. Second, the drag coefficient C_{Da} for a cylinder array can be calculated simply using the classical C_D-R relationship for an isolated cylinder. The calculation can proceed with the following steps. First, R' is calculated using Eq. (28). Then, C_D' is calculated using Eq. (29) [the same function as Eq. (1)]. Next, C_{Da} is found from Eq. (27) with C_D', S, and λ.

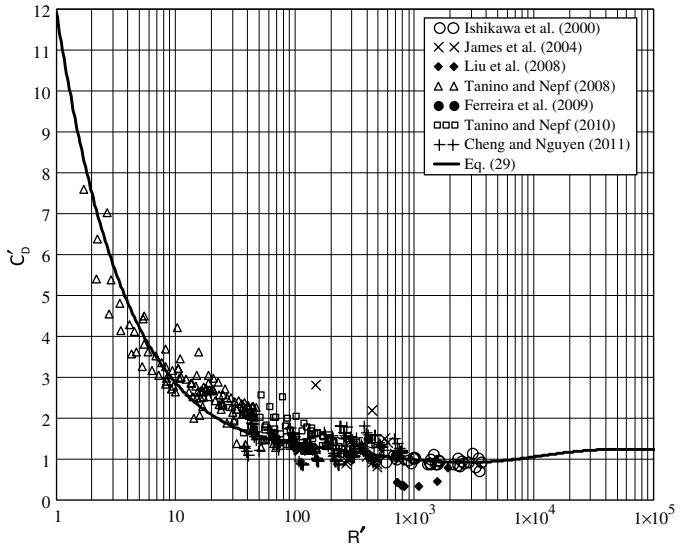

Fig. 7. Generalized relationship between drag coefficient C_D' and Reynolds number R' for different vegetation configurations, where $C_D' = (1-\lambda)C_{Da}/(1+S)$ and $\mathsf{R}' = (1+S)R_a/(1+80\lambda)$

Discussions

By applying the procedure proposed, the average flow velocity (V_v) through the emergent vegetation can be calculated from the measurements of vegetation configuration (λ and d), energy slope (S), and fluid viscosity (ν). In this procedure, it is assumed that the energy slope is known, which is true for laboratory experiments. For field applications, V_v may be measured directly, and S (and thus the vegetation-induced drag) is to be calculated. For such cases, the calculation could be done either using Eq. (12) [together Eqs. (20) and (21)] or Eq. (29) [together Eqs. (21) and (28)]. However, by noting that S is included in d_*', R', and C_D', iterations are needed.

It has been shown that the database of the measured flow velocities through the emergent vegetation can be well represented using the formula that is derived based on the pseudofluid concept. However, the approach does not involve any analysis of stem-induced flow phenomena such as eddy–eddy and eddy–stem interactions. Such flow information is essential for a physics-based formulation of the apparent viscosity. The linear viscosity function [Eq. (24)] proposed in this study, though workable for the model, is empirical and may need further improvements.

In this study, the consideration is limited to the emergent vegetation simulated using rigid cylindrical rods. For the case of natural vegetation, the geometrical shape and the flexibility of the stem may become major factors to be considered in developing an approach to evaluation of the drag. Though not included in the current approach, the factors could be investigated using a method similar to that presented in this paper. This could be done by first considering the drag that is induced by a single stem of particular shape and/or flexibility. Then the evaluation of the drag, once known for a single stem, could be further extended to an array

of the same stems with varying configurations. Such an investigation is worth future efforts.

In Cheng and Nguyen (2011), the vegetation-based hydraulic radius (r_v) is used as a length scale to replace the cylinder diameter in defining Reynolds number, which yields a good relationship between the drag coefficient (C_{Da}) and the Reynolds number ($r_v V_v/\nu$). It is also shown that the relationship does not vary with the vegetation fraction (λ). Alternatively, this relationship is reformulated in the present study [see Eq. (29)] using the different definitions of the drag coefficient and Reynolds number (i.e., C_D' and R'). Being different from the previous result, the new relationship can be reduced for the sparse case to the classical function [e.g., Eq. (1)] that is established for a single isolated cylinder subject to a cross flow.

Summary

In this study, the vegetation-induced drag in an open-channel flow is first compared to that caused by a settling cylinder array. This yields that the relevant energy slope observed in the open-channel flow is related to the relative density difference that drives the settling. Then a pseudofluid model is established to extend the drag coefficient relation that is used for an isolated cylinder to the condition in the presence of multiple cylinders. The analysis shows that the vegetation fraction has significant effects on the drag coefficient for a given Reynolds number, in particular at low Reynolds numbers, which is in good agreement with experimental observations. Moreover, the vegetation fraction effect can be incorporated simply by parameterizing the drag coefficient and Reynolds number based on the pseudofluid concept. The analytical model was calibrated using the experimental data available in the literature. Simple procedures that are useful for practical applications are proposed for predicting the drag coefficient for the cylinder array and the average flow velocity through it. The analysis presented in this study is limited to the emergent, rigid, identical cylinders.

Appendix. Calculation of V_v and Its Approximation

Consider an equilateral triangle formed by three cylinders (see Fig. 8). For this simplified bed configuration, the cylinder-occupied bed area is $\pi d^2/4$ in the rectangle denoted by the dotted line, and thus the average solid fraction λ is $(\pi/\sqrt{12})(d/s)^2$, where s is the distance between the two neighboring cylinders. However, the cross-sectional solid fraction varies in the streamwise or x-direction, which can be expressed as

$$\phi(x) = \begin{cases} \frac{2}{s}\sqrt{\left(\frac{d}{2}\right)^2 - x^2} & \text{if } 0 \le x \le \frac{d}{2} \\ 0 & \text{if } \frac{d}{2} < x \le L - \frac{d}{2} \\ \frac{2}{s}\sqrt{\left(\frac{d}{2}\right)^2 - (L-x)^2} & \text{if } L - \frac{d}{2} < x \le L \end{cases} \tag{30}$$

where $L = (\sqrt{3}/2)s$. It can be shown that for $L/d > 1$ or $s/d > 1.15$, the average of $\phi(x)$ over the rectangular bed area is equal to λ. If the flow depth h is constant and independent of x, the average flow velocity V_v through the emergent cylinders can be generally expressed as

$$V_v = \beta \frac{Q}{Bh} \tag{31}$$

where

$$\beta = \frac{1}{L}\int_0^L \frac{1}{1-\phi(x)}\,dx \tag{32}$$

Obviously, β is dependent on the cylinder configuration. For simplicity, if assuming that $\phi(x) = \lambda$, β becomes constant and is equal to

$$\beta_o = \frac{1}{1-\lambda} \tag{33}$$

Then, the average velocity V_v is estimated as $Q/[Bh(1-\lambda)]$, as done in some previous studies [e.g., Tanino and Nepf (2008), Kothyari et al. (2009a), and Cheng and Nguyen (2011)]. However, this calculation is considered only as an approximation by noting that β is generally not the same as β_o. Fig. 9 shows that the difference between β and β_o, which is calculated for the simplified bed configuration given in Fig. 8, is less than 4.5% if $\lambda < 15\%$ or $s/d > 2.5$. Therefore, the approximation of $\beta = \beta_o$ is acceptable for $\lambda < 15\%$, which applies to six of the seven sources of data summarized in Table 1. The exceptional data set is the one reported by Tanino and Nepf (2008), who employed randomly distributed cylinders with λ ranging from 9 to 35%. For this set of data, if λ is higher than 15%, the average velocities estimated using Eq. (31) could become larger than those by taking $\beta = \beta_o$. However, detailed results cannot be obtained because the information about $\phi(x)$ is not available for randomly distributed cylinders.

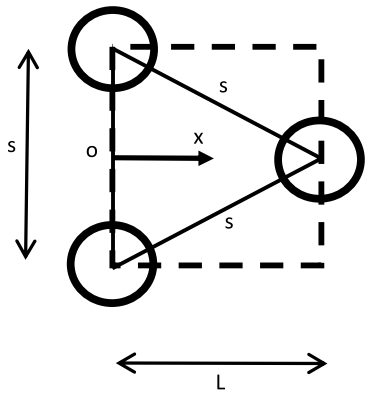

Fig. 8. Simplified cylinder configuration

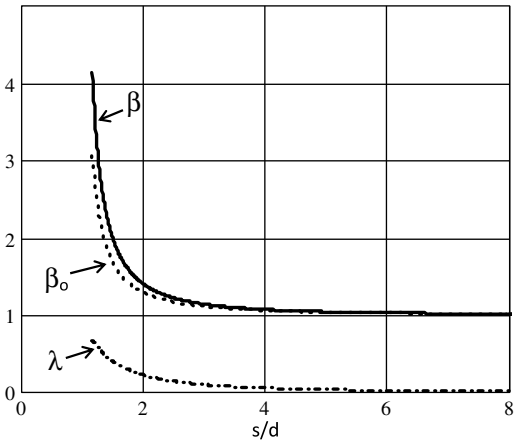

Fig. 9. Difference between β and β_o

J. Hydraul. Eng., 2013, 139(6): 602-611

Acknowledgments

This study was partially supported by the Open Fund of the State Key Laboratory of Hydraulics and Mountain River Engineering, Sichuan University, Chengdu, P. R. China. The author is grateful to the comments and suggestions, provided by the reviewers and editors, which yield significant improvements in the presentation of the results obtained.

Notation

The following symbols are used in this paper:

B = channel width;
C_D = drag coefficient for isolated cylinder;
C_{Da} = drag coefficient for cylinder array;
C'_D = drag coefficient for pseudofluid model;
d = cylinder diameter;
d_* = dimensionless cylinder diameter defined as $(2C_D\mathsf{R}^2/\pi)^{1/3}$;
d'_* = dimensionless cylinder diameter defined as $(2C'_D\mathsf{R}'^2/\pi)^{1/3}$ for pseudofluid model;
Err_1 = average relative error;
Err_2 = average squared deviation defined using logarithmic velocity;
F_D = average drag acting on an isolated cylinder per unit length;
F_{Da} = average drag acting on a cylinder per unit length in cylinder array;
f = friction factor $(= 8grS/V_v^2)$;
f_b = bed-related friction factor;
f_w = sidewall-related friction factor;
g = gravitational acceleration;
h = flow depth;
N = total number of cylinders in control volume;
Q = flow discharge;
R = Reynolds number defined as Vd/ν for an isolated cylinder;
R_a = Reynolds number defined as $V_v d/\nu$ for cylinder array;
R' = Reynolds number defined as $V_v d/\nu'$ for pseudofluid model;
r = hydraulic radius defined in Eq. (26);
r_v = vegetation-based hydraulic radius defined as $\pi(1-\lambda)d/(4\lambda)$;
r_{vm} = modified vegetation-based hydraulic radius (due to sidewall correction);
S = energy slope in open channel flow;
V = average velocity of a cross flow;
V_v = average velocity through emergent vegetation calculated as $Q/(Bh(1-\lambda))$;
W = effective weight of cylinder per unit length;
X = length of control volume;
Y = width of control volume;
Z = height of control volume;
α = constant;
Δ = relative density difference defined as $(\rho_s-\rho)/\rho$;
Δ' = relative density difference defined as $(\rho_s-\rho')/\rho'$ for pseudofluid model;
λ = vegetation fraction or fraction of stem-occupied bed area;
μ = dynamic viscosity of fluid;
μ_r = relative dynamic viscosity defined as μ'/μ;
μ' = apparent dynamic viscosity of pseudofluid;
ν = kinematic viscosity of fluid;
ν_r = relative kinematic viscosity defined as ν'/ν;
ν' = apparent kinematic viscosity of pseudofluid;
ρ = fluid density;
ρ_s = density of cylinder for pseudofluid model; and
ρ' = apparent density of pseudofluid.

References

Baptist, M. J., et al. (2007). "On inducing equations for vegetation resistance." *J. Hydraul. Res.*, 45(4), 435–450.
Cheng, N. S. (1997). "Effect of concentration on settling velocity of sediment particles." *J. Hydraul. Eng.*, 123(8), 728–731.
Cheng, N. S. (2011). "Representative roughness height of submerged vegetation." *Water Resour. Res.*, 47(W08517), 1–18.
Cheng, N. S., and Chiew, Y. M. (1999). "Incipient sediment motion with upward seepage." *J. Hydraul. Res.*, 37(5), 665–681.
Cheng, N. S., and Law, A. W. K. (2003). "Exponential formula for computing effective viscosity." *Powder Technol.*, 129(1–3), 156–160.
Cheng, N. S., and Nguyen, H. T. (2011). "Hydraulic radius for evaluating resistance induced by simulated emergent vegetation in open-channel flows." *J. Hydraul. Eng.*, 137(9), 995–1004.
Cheng, N. S., Nguyen, H. T., Tan, S. K., and Shao, S. D. (2012). "Scaling of velocity profiles for depth-limited open channel flows over simulated rigid vegetation." *J. Hydraul. Eng.*, 138(8), 673–683.
Clift, R., Grace, J. R., and Weber, M. E. (1978). *Bubbles, drops, and particles*, Academic Press, New York.
Einstein, A. (1906). "A new determination of the molecular dimensions." *Annalen Der Physik*, 324(2), 289–306.
Ferreira, R. M. L., Ricardo, A. M., and Franca, M. J. (2009). "Discussion of 'Laboratory investigation of mean drag in a random array of rigid, emergent cylinders' by Yukie Tanino and Heidi M. Nepf." *J. Hydraul. Eng.*, 135(8), 690–693.
Finn, R. K. (1953). "Determination of the drag on a cylinder at low Reynolds numbers." *J. Appl. Phys.*, 24(6), 771–773.
Gibilaro, L. G. (2001). *Fluidization-dynamics: The formulation and applications of a predictive theory for the fluidized state*, Butterworth-Heinemann, Oxford, UK.
Gibilaro, L. G., Gallucci, K., Di Felice, R., and Pagliai, P. (2007). "On the apparent viscosity of a fluidized bed." *Chem. Eng. Sci.*, 62(1–2), 294–300.
Huthoff, F., Augustijn, D. C. M., and Hulscher, S. J. M. H. (2007). "Analytical solution of the depth-averaged flow velocity in case of submerged rigid cylindrical vegetation." *Water Resour. Res.*, 43(6), W06413, 1–10.
Ishikawa, Y., Mizuhara, K., and Ashida, S. (2000). "Effect of density of trees on drag exerted on trees in river channels." *J. For. Res.*, 5(4), 271–279.
James, C. S., Birkhead, A. L., Jordanova, A. A., and O'Sullivan, J. J. (2004). "Flow resistance of emergent vegetation." *J. Hydraul. Res.*, 42(4), 390–398.
Jayaweera, K. O. L. F., and Mason, B. J. (1965). "The behaviour of freely falling cylinders and cones in a viscous fluid." *J. Fluid Mech.*, 22(4), 709–720.
Jordanova, A. A., and James, C. S. (2003). "Experimental study of bed load transport through emergent vegetation." *J. Hydraul. Eng.*, 129(6), 474–478.
Kothyari, U. C., Hashimoto, H., and Hayashi, K. (2009a). "Effect of tall vegetation on sediment transport by channel flows." *J. Hydraul. Res.*, 47(6), 700–710.
Kothyari, U. C., Hayashi, K., and Hashimoto, H. (2009b). "Drag coefficient of unsubmerged rigid vegetation stems in open channel flows." *J. Hydraul. Res.*, 47(6), 691–699.
Kouwen, N., Unny, T. E., and Hill, H. M. (1969). "Flow retardance in vegetated channels." *J. Irrig. Drain. Div.*, 95(2), 329–342.
Kundu, P. K., Cohen, I. M., and Hu, H. H. (2004). *Fluid mechanics*, Elsevier Academic, Amsterdam, The Netherlands.
Lamb, H. S. (1945). *Hydrodynamics*, Dover Publications, New York.
Liu, D., Diplas, P., Fairbanks, J. D., and Hodges, C. C. (2008). "An experimental study of flow through rigid vegetation." *J. Geophys. Res. Earth Surf.*, 113, F04015, 1–16.

Luhar, M., Rominger, J., and Nepf, H. (2008). "Interaction between flow, transport and vegetation spatial structure." *Environ. Fluid Mech.*, 8(5–6), 423–439.

Nepf, H., Ghisalberti, M., White, B., and Murphy, E. (2007). "Retention time and dispersion associated with submerged aquatic canopies." *Water Resour. Res.*, 43(4), W04422, 1–10.

Nepf, H. M. (1999). "Drag, turbulence, and diffusion in flow through emergent vegetation." *Water Resour. Res.*, 35(2), 479–489.

Niemann, H. J., and Holscher, N. (1990). "A review of recent experiments on the flow past circular-cylinders." *J. Wind Eng. Ind. Aerodyn.*, 33(1–2), 197–209.

Poletto, M., and Joseph, D. D. (1995). "Effective density and viscosity of a suspension." *J. Rheol.*, 39(2), 323–343.

Stone, B. M., and Shen, H. T. (2002). "Hydraulic resistance of flow in channels with cylindrical roughness." *J. Hydraul. Eng.*, 128(5), 500–506.

Sumer, B. M., and Fredsøe, J. (1997). *Hydrodynamics around cylindrical structures*, World Scientific, Singapore.

Tanino, Y., and Nepf, H. M. (2008). "Laboratory investigation of mean drag in a random array of rigid, emergent cylinders." *J. Hydraul. Eng.*, 134(1), 34–41.

Tritton, D. J. (1959). "Experiments on the flow past a circular cylinder at low Reynolds numbers." *J. Fluid Mech.*, 6(4), 547–567.

Wan, Z., and Wang, Z. (1994). *Hyperconcentrated flow*, A.A. Balkema, Rotterdam, The Netherlands.

Wieselsberger, C. (1922). "New data on the laws of fluid resistance." *Technical Note No. 84*, National Advisory Committee for Aeronautics, Washington, DC.

Williamson, C. H. K. (1996). "Vortex dynamics in the cylinder wake." *Annu. Rev. Fluid Mech.*, 28(1), 477–539.

Zdravkovich, M. M. (1997). *Flow around circular cylinders: A comprehensive guide through flow phenomena, experiments, applications, mathematical models, and computer simulations*, Oxford University Press, Oxford, UK.